Earth`s Cryosphere, 2018, vol. XXII, No. 5, pp. 67–84 **http://earthcryosphere.ru/**

DOI: 10.21782/EC2541-9994-2018-5(67-84)

PERMAFROST STUDY IN THE NORTHERN MARGIN OF THE SIBERIAN PLATFORM BASED ON REGIONAL GEOELECTRICAL SURVEY DATA

D.V. Yakovlev[1], A.G. Yakovlev[1,2], O.A. Valyasina[2]

[1] *Nord-West Ltd., korpus A, Business centre "Rumyancevo", pos. Moskovskiy, Moscow, 108811, Russia; nw.yakovlev@gmail.com*
[2] *Lomonosov Moscow State University, Faculty of Geology, 1, Leninskie Gory, Moscow, 119991, Russia*

The paper presents results of the permafrost study in the northern margin of the Siberian Platform, obtained during regional geoelectrical surveys by magnetotelluric and transient electromagnetic methods. The surveys aimed to identify areas perspective for oil and gas within the entire sedimentary cover. In the period from 2005 to 2016, more than 30,000 soundings were performed with a total survey line length of more than 20,000 km. A large amount of factual data acquired in the Yenisei-Khatanga and the Anabar-Lena regional troughs allowed mapping the permafrost base depth and provided insights about other structural features of the permafrost interval, along with the information on permafrost distribution beneath the Khatanga Bay. High-resistivity anomalies identified above the hydrocarbon-bearing reservoirs capped by the permafrost strata are likely to be associated with accumulations of gas-hydrates.

Electromagnetic, magnetotelluric soundings, transient electromagnetic sounding, permafrost, cryolithozone, gas hydrates, Yenisei-Khatanga trough, Anabar-Lena trough

INTRODUCTION

Electrical resistivity measurements as part of electrical prospecting is an effective method in permafrost studies [*Zykov, 1999; Yakupov, 2008*], inasmuch as conductivity of sedimentary rocks is determined mainly by the presence of water in the pore space, while, when freezing, this water produces a many-fold increase in electrical resistivity (ER) of sediments [*Ogil'vi, 1990*].

Traditionally used diverse electric prospecting methods in permafrost studies include: various modifications of direct current (DC) and alternating current (AC) resistivity prospecting methods, time-domain or transient electromagnetic sounding (TEM) and frequency-domain sounding. Magnetotelluric (MT) soundings are often applied to investigations of deeper subsurface. MT surveys have been known as appropriate for permafrost studies since the 70s of the last century [*Koziar and Strangway, 1975*], mainly in the high-frequency modification [*Koziar and Strangway, 1978*].

The intensive regional geophysical investigations have been conducted within the northern margin of the Siberian platform with an aim to identify new zones of oil/gas accumulation since 2004. The study area comprises the territory of Gydan and Taimyr peninsulas, and the interfluve of the Khatanga and Lena rivers, whose tectonic structure is represented by such major elements, as the Taimyr folded system, Yenisei-Khatanga regional trough (Yenisei-Khatanga basin) and Anabar-Lena trough (Anabar-Lena basin) (Fig. 1).

Seismic prospecting (common depth point method) and magnetotelluric (MT) soundings as part of the electrical prospecting technique form the basis of the integrated geophysical surveys aimed at revealing specific features of the composition and structure of Jurassic-Cretaceous strata and Paleozoic complexes [*Afanasenkov and Yakovlev, 2018*]. While the results derived from the regional MT profile network showed that the new-generation MT sounding technique is almost as good for the study of geological structure of the permafrost zone by ensuring effective measurements of the thickness of perennially frozen sediments (permafrost), determination of their structural heterogeneity and detection of subpermafrost anomalies which can be associated with hydrocarbons (HC).

We consider it necessary to remind the readers of some definitions of the geocryological terms used in this paper: *perennially frozen deposits* (or permafrost) are deposits which have negative temperatures, with at least part of the pore moisture turned to ice; deposits which have negative temperatures, with the unfrozen pore moisture are interpreted as "*unfrozen*" or "*cooled*". The term c*ryolithozone (permafrost zone)* is defined as "the zone of the occurrence of deposits with negative temperatures which may remain unfrozen given sufficient salinity of pore water solutes, however, when affected by the processes leading to further decrease in their temperature they will be refreezing" [*Yakupov, 2008*]. Given that resistivity of deposits increases sharply when water transitions from liquid to solid state, permafrost deposits are distinctly distinguished in the electrical resistivity profile against the backdrop of unfrozen (cooled) deposits. At this, resistivity of the permafrost-related portion of deposits in the unfrozen/cooled state may be no different from that of the sediments occurring beneath the permafrost strata.

Copyright © 2018 D.V. Yakovlev, A.G. Yakovlev, O.A. Valyasina, All rights reserved.

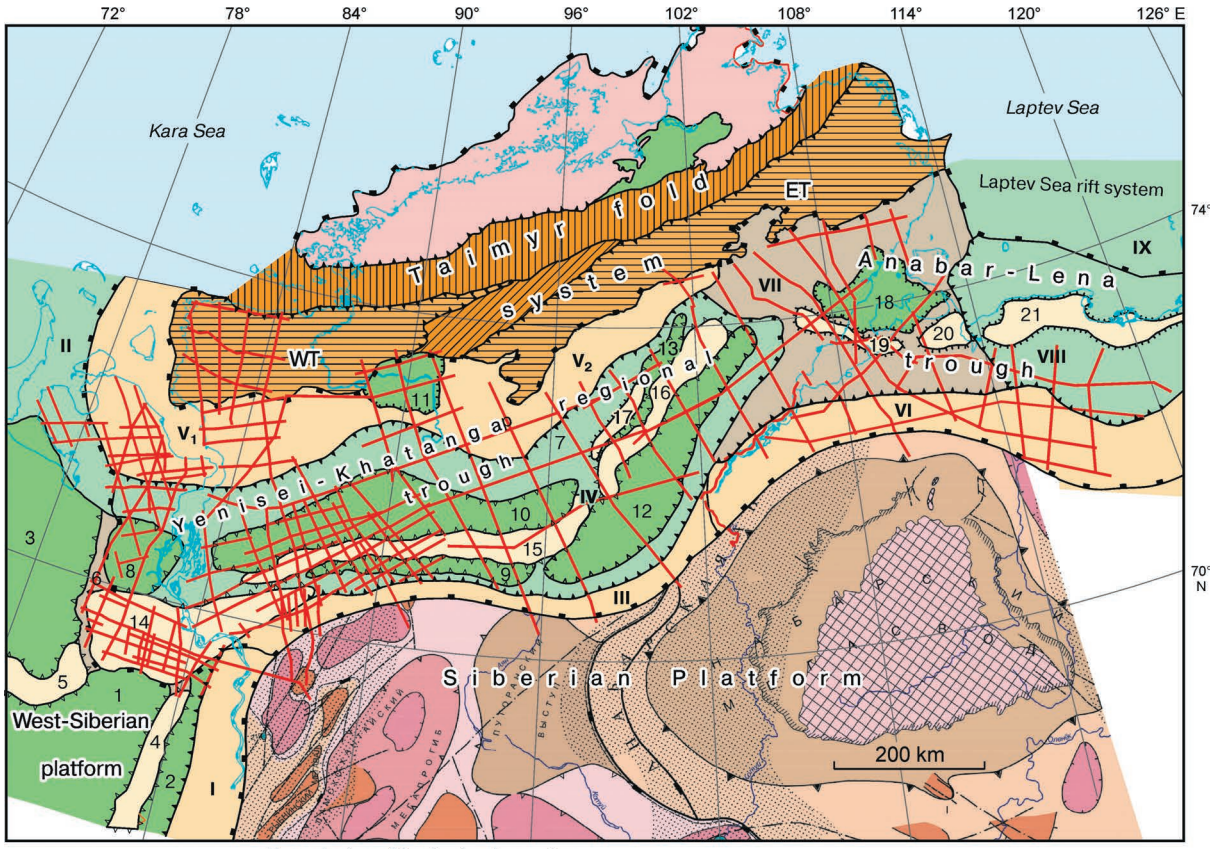

Boundaries of tectonic elements:

high-rank order
superorder
I order
II order
Scoastline
MT profiles

Taimyr fold system:

Paleozoic depressions
WT – West Taimyr
ET – East Taimyr
Tarey swell
Bordering flexure
Schrenk half-graben
North-Taimyr Shield

West-Siberian platform:

Superorder elements:
I – Pakulikha minicline
II – Yamal-Gudan transition area

I order:

Negative:
1. Pendomayakha depression
2. Dolgan trough
3. Yamal-Gydan syneclise

Positive:
4. Suzun-Vankor swell
5. Messoyakha megaswell
6. Gydan saddle

Structural-tectonic elements in Mesozoic deposits:

positive
II negative superorder
negative I order and II order
VI monoclines and uplifts
VII saddles

Yenisei-Khatanga regional trough:

Superorder elements:
III – North-Siberian monocline
IV – Central Taimyr trench
V – Taimyr monocline
V_1 – South-Taimyr monocline
V_2 – Jangoda-Gorbit uplift

I order and II order:

Negative:
7. Gydan-Khatanga transition area
8. Nosok trough
9. Dudypta megatrough
10. Agapa megatrough
11. Pyasina half-graben
12. Boganid-Zhdanikha megatrough
13. Turku-Logata trough

Positive:
14. Tanama-Malaya Kheta megaswell
15. Rassokha megaswell
16. Balakhna megaswel
17. Kubalakh megaswell

Siberian Platform:

positive
negative
Major regional faults
Zones of intense Riphean subsidence

Anabar-Lena trough:

Superorder elements:
VI – Anabar monocline
VII – Anabar-Khatanga saddle
VIII – Lena-Anabar depression

I order and II order:

Negative:
18. Kharatumus depression

Positive:
19. Sopochnaya uplift zone
20. Nordvik swell
21. Tyagin-Anabar uplift zone

Laptev Sea rift system:

Superorder elements:
IX – South-West Laptev Sea depression

Fig. 1. Position of the magnetotelluric sounding profiles on the structural-tectonic map of the northern framing of the Siberian platform [*Afanasenkov et al., 2018*].

In practical applications, the information about the structure of permafrost strata represents the greatest interest both from the perspective of geological engineering tasks, and in estimation of the shallow subsurface effect on the of seismic survey results.

RESISTIVITY PROSPECTING TECHNIQUE

Of the AC resistivity prospecting methods, the MT sounding technique is largely premised on the study of the Earth's natural electromagnetic field [*Berdichevskii and Dmitriev, 2009*]. The MT soundings were carried out in a wide frequency range from 0.0003 to 300 Hz using state-of-the-art equipment produced by Phoenix Geophysics Ltd, Canada. The measurements included: electric field components (using grounded electric dipoles), and magnetic field components (using induction sensors). In the early years (2004 through 2009), the regional works were performed with 2–3 km spacing along the profile, which soon was narrowed to 1 km, while the surveys were spaced at 500 m intervals within the bounds of Novotaimyrskaya area in 2014–2015.

The transient electromagnetic (TEM) method, another resistivity prospecting technique, which is complementary to MT soundings, allows to effectively study the permafrost interval through its full thickness. TEM soundings enable investigation of the field of transient processes occurring in the subsurface when a DC current injected into the loop is abruptly turned off [*Khmelevskoy and Kostitsin, 2010*]. The transmitter/receiver configurations commonly include either loops or electric dipoles, designated for the surface and marine geophysical investigations, respectively. The use of ungrounded loops for signal excitation and receiving in the TEM method allows simplifying the field work methods in winter conditions and avoidsing distortion caused by near-surface inhomogeneities. Noteworthy is the problem arising with the induced polarization (fast-decaying IP, or Maxwell–Wagner effect) appearing on TEM curves for permafrost deposits [*Ageev and Ageev, 2017*]. Suppression of this effect involves the need for complicating the field work techniques and using measuring and transmitter loops spaced apart.

Given that the solution of the posed geological tasks required depths inaccessible by the TEM method in the study area, the MT soundings were used as a basic technique. At this, the data on the permafrost structure were obtained from regional MT sounding as additional information. The results and conclusions presented in the paper are therefore largely based on the MT sounding data, which might as well be obtained from TEM sounding results [*Nim et al., 1994; Baranov et al., 2014*].

In 2014–2015, the MT soundings on some of the regional profiles were coupled with TEM surveys, which offered an opportunity to compare the results of the two electrical prospecting methods. On these profiles, TEM soundings were aimed at suppressing the effect of near-surface inhomogeneities on the MT sounding results. As such, the integration of TEM and MT soundings is used in industry worldwide [*Sternberg et al., 1988*]. Figure 2 presents geoelectric sections obtained from TEM and MT soundings along one of the profiles. The sections were constructed independently for each method based on the results of 1D Occam's inversion of the MT data [*Constable et al., 1987*]. The comparison of these sections revealed similarity between the results obtained by the two different methods, which is also corroborated by identical local anomalies patterns and their regional constituent.

Geoelectrical characteristics of the shallow subsurface

Most of the Mesozoic-Cenozoic deposits of the Yenisei-Khatanga and Anabar-Lena basins are composed by sands, sandstones, mudstones and siltstones, which make up the gently occurring grey terrigenous sequence varying from 10 to 12 km in thickness in the axial parts of the troughs to zero in their sides [*Afanasenkov et al., 2018*].

Results of electrical resistivity prospecting. The results of electrical resistivity surveys of terrigenous Jurassic-Cretaceous deposits in a normal environment yielded the average of 7–30 Ohm·m. The resistivities being relatively low in this interval of the section is accounted for by the presence of water in the deposits owing to their high effective porosity.

All the geoelectrical sections have demonstrated that the upper several hundred meters within the study area have high resistivities varying from 100 to 500 Ohm·m (Fig. 2), which proves it to be a high-resistivity, very heterogeneous layer, with its thickness varying from 0 to 600 m, and reaching locally up to 1100 m. In places where Mesozoic-Cenozoic deposits outcrop on the surface, this layer corresponds to the permafrost deposits. Given that higher resistance is inherent both in Paleozoic deposits and Permian-Triassic flood basalts (Fig. 2), this makes it difficult to identify permafrost deposits in their resistivity profiles.

Note that with the resistivity measured by DC electrical prospecting methods, the permafrost deposits are characterized by values of thousands of Ohmmeters. While when the induction electromagnetic prospecting methods are involved, which include MT and TEM soundings, the obtained resistivities of permafrost deposits will be several times lower. This striking difference can be explained by the effect of anisotropy [*Khmelevskoy et al., 2005*]. In the case of insulator layers, by themselves representing subhorizontal alternation of layers with different resistance, resistivity will be determined mainly from longitudinal conductance of lower-resistivity layers in the case

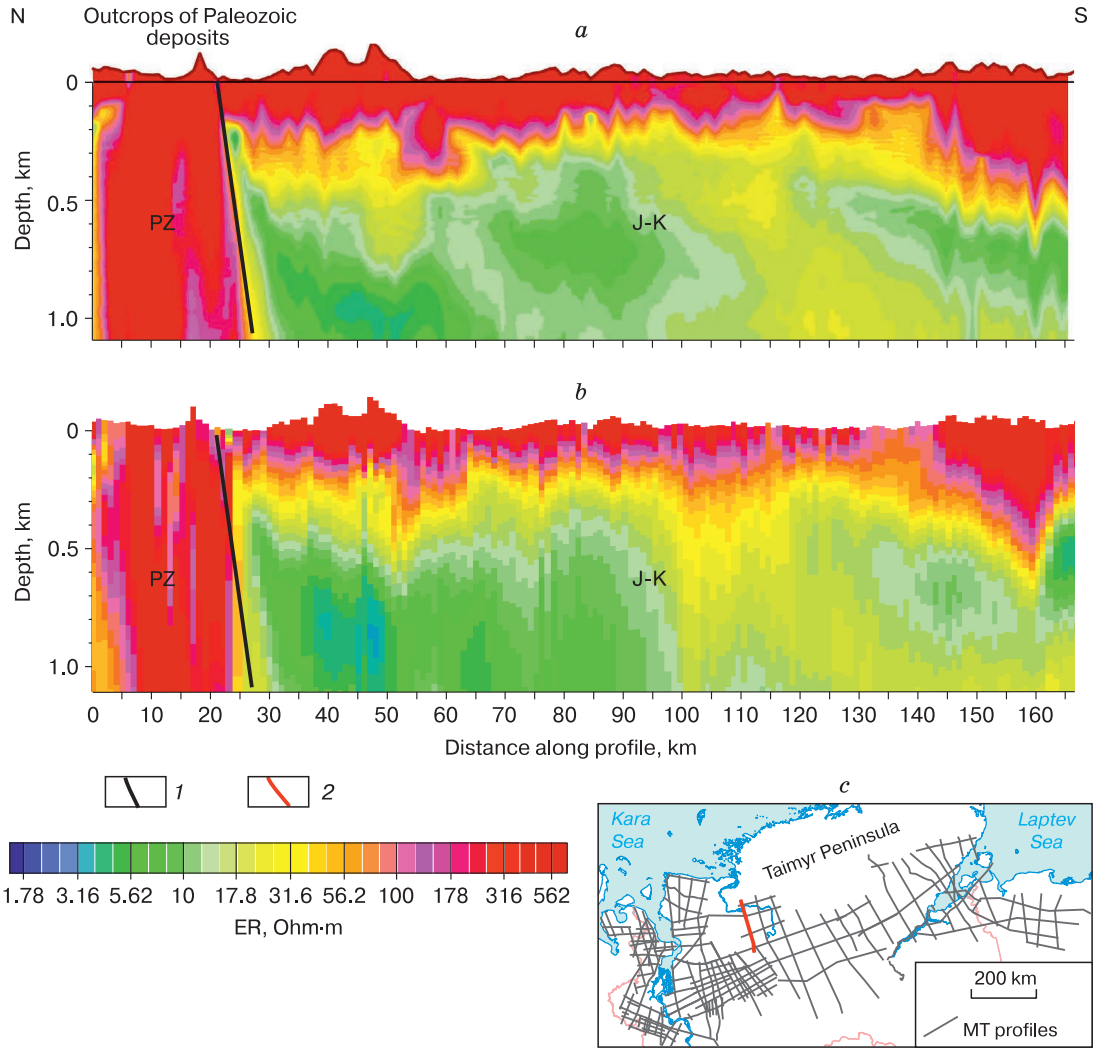

Fig. 2. Comparison of geoelectric sections built from the same profile according to TEM (*a*) and MT soundings (*b*) and the scheme of regional electric prospecting profiles of the study area (*c*).

Geological complexes: PZ – Paleozoic, J–K – Jurassic-Cretaceous. The profile spacing: *a* – 500 m; *b* – 1000 m. *1* – tectonic boundary between geological complexes derived from the electrical resistivity measurements; *2* – the profile position on the scheme.

of application of induced polarization methods, and from transverse resistance of higher resistivity layers when using DC (galvanic) methods.

Comparison of results with the electrical well logging. Figure 3 presents a type geoelectric section inferred from the MT sounding data to a depth of 2 km along the profile striking roughly W–E in the Yenisei-abutting stretch of the Yenisei-Khatanga basin. The section resulted from the simple automatic one-dimensional inversion of the effective MT curves $Z_{\text{eff}} = (Z_{xx}Z_{yy} - Z_{xy}Z_{yx})^{1/2}$ [*Berdichevskii and Dmitriev, 2009*]. The thickness of high resistivity layer assumingly corresponding to permafrost deposits changes significantly on this profile: from 50 m with in the Yenisei river area up to 450 m in eastern part of the profile exhibiting a local thickness anomaly of up to 700 m in the Rassokha megaswell area. The revealed good agreement between resistivities inferred from the MT soundings and electrical borehole logs is also characteristic of the entire study area (Fig. 4). Electrical resistivities of permafrost deposits determined from the logs vary from 100 to 1000 Ohm·m.

Judging from the results of borehole temperature measurements, the permafrost thickness averages 450–550 meters in this area. Given that the thermometric measurements are often performed in unstable wells (with unsteady thermal regime) (BH 1, 4, 5 in Fig. 4), this makes obtaining absolute temperature values extremely difficult. In wells showing no transition from negative to positive values on the tempera-

ture curve, the permafrost strata is therefore interpreted to be within the T curve segment containing a zero or weak temperature gradient, while the permafrost base (lower boundary) is discriminated by a transition from a zero or weak to normal geothermal gradient (3 °C per 100 m) (Fig. 4). This determination method reduces the level of confidence of the values obtained, though.

The thickness of permafrost and the depth of its distribution derived from the results of electrical prospecting show close proximity in eastern part of the section (Fig. 3), while they differ significantly in the west, which is accounted for the westward trend of the cooled deposits distribution in the lower part of the permafrost interval. The reason why pore moisture in the permafrost deposits is found unfrozen, can probably be explained either by higher salinity of pore water solutes, or the predominance of clayey sediments in the section. Below we consider each of these reasons individually.

Pore water salinity. With little data available on salinity (total dissolved solids, TDS) of pore water solutes, the available data indicate (Fig. 5) that the measured water salinity averaging 6–8 g/L almost everywhere in the near-surface section is, in fact, significantly lower than typical sea water salinity of 30–35 g/L, freezing at –1.8 °C and below. While higher TDS values (up to 22 g/L) reported from some wells are likely associated with rejection of salts beneath the permafrost layer in the process of water crystallization [*Romanovsky, 1983*]. The zones of enhanced salinity of pore water solutes on the geoelectric sections may manifest themselves as patches of very low resistivity overlain by the layer of high-resistivity permafrost deposits. They are observed, for example, westward of the Yenisei river at a depth of 150–200 m (Fig. 3), being representative however of individual localities. While weakly saline pore solutes generally found everywhere do not allow to tie up the observed region-specific changes in permafrost thickness with variations of pore moisture salinity.

It should be noted that a relatively low salinity of pore water solutes allows (according to the calculations performed by A.A. Ryzhov for sandy-clayey Jurassic-Cretaceous sediments) differentiating essentially clayey from sandy layers by resistivity [*Ryzhov and Sudoplatov, 1990*]. At salinity less than 10–15 g/L, other conditions being equal, clays have a lower resistivity than sands and sandstones, which proved critical in constructing lithological columns

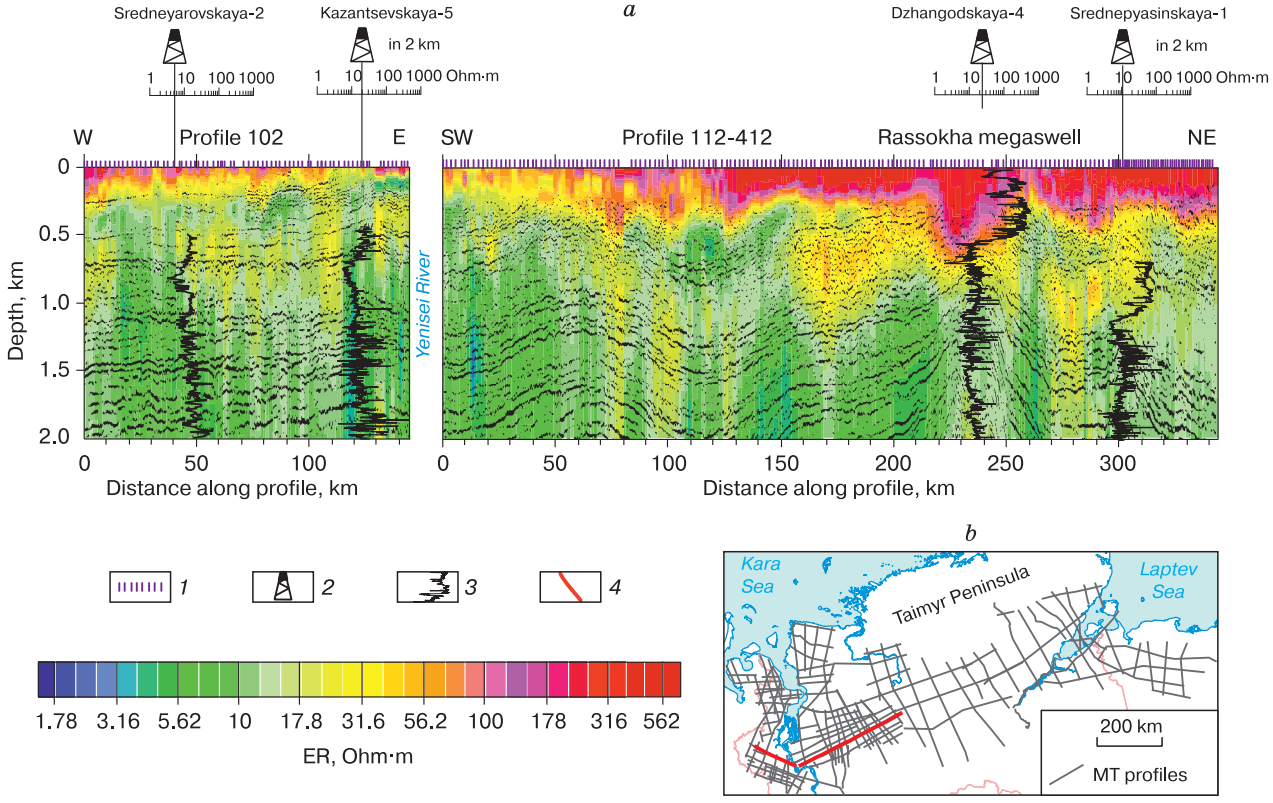

Fig. 3. Characteristic geoelectric section to a depth of 2 km according to MT sounding data in the western part of the Yenisei-Khatanga basin (*a*) and the scheme of regional electric prospecting profiles for the study area (*b*).

1 – MT sounding points; *2* – deep drilled wells; *3* – resistivity logs from wells; *4* – profile position on the scheme.

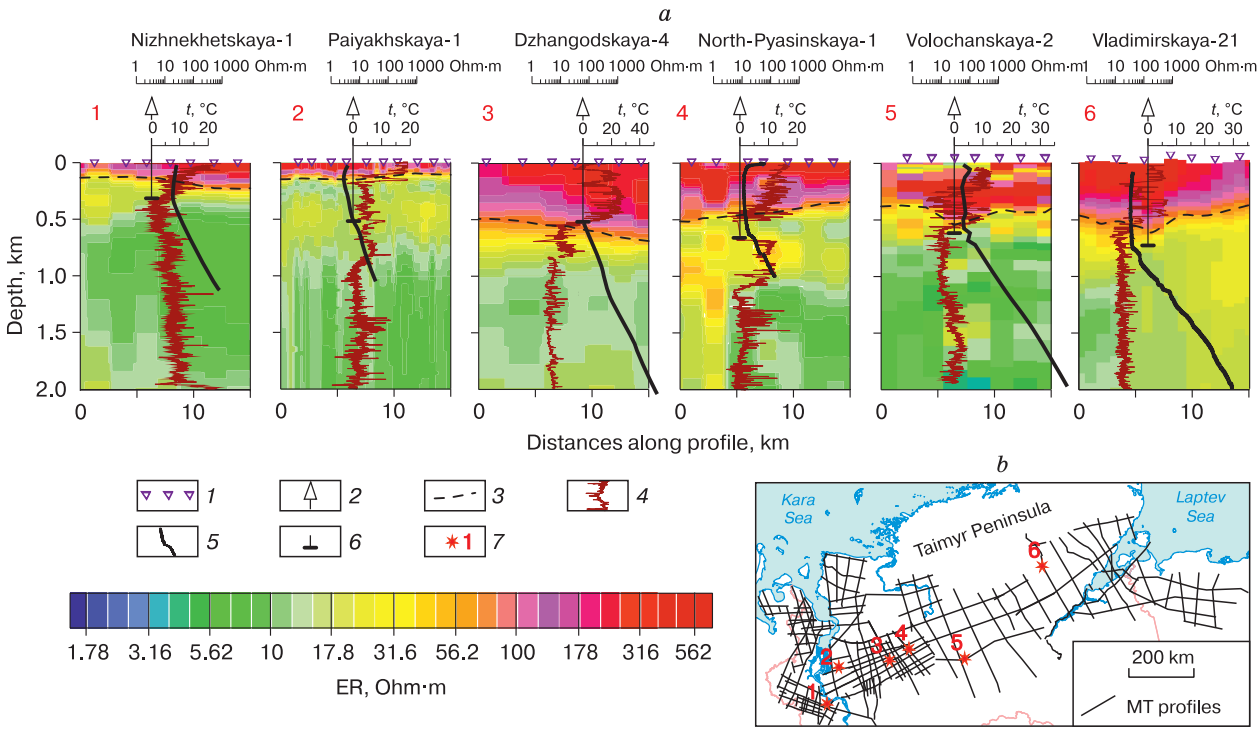

Fig. 4. Comparison of geoelectric sections with the well log data (*a*) and the scheme of regional electric prospecting profiles for the research area (*b*).

1 – points MT sounding; *2* – the position of wells on the profile; *3* – the position of the base of frozen deposits according to MT sounding; *4* – diagrams logging resistivity in wells; *5* – thermometry curve; *6* – the base of the permafrost thermometry; *7* – the position and number of wells in the scheme.

of the Jurassic-Cretaceous complex of the Yenisei-Khatanga basin from the electrical prospecting data [*Afanasenkov and Yakovlev, 2018*].

Clayey permafrost deposits. The wide distribution of cooled deposits in the permafrost zone can be explained by the predominance of clayey deposits in the section. The clays contain large amounts of bound water, freezing at a temperature lower, than free water. As a result, all other things being equal, resistivity of sand deposits changes abruptly as the temperature crosses over the "freezing point of the pore water solute", while that of clayey deposits has a smoother pattern at lower temperatures (Fig. 6) [*Ogil'vy, 1990*]. Besides, the contrast between the resistivity of sands (ρ_s) and clays (ρ_c) increases significantly during their transition from the cooled to the frozen state (Fig. 6). Note that dependencies shown in Fig. 6 reflect resistivities of either freezing deposits or those having stable temperature values. The resistivity measured in the thawing deposits changes with a "delay", forming thereby a kind of hysteresis loop. Nevertheless, the sand to clay resistivities ratio is preserved. These patterns of changes in the electrical resistivity of negative-temperature deposits account for the structural features of permafrost strata inferred from the electrical resistivity data for the study area.

Specifically, the high clayey content of permafrost deposits explains a significant difference between the thicknesses of the permafrost strata and the permafrost zone in the west of the study area (the Yenisei-abutting stretch of the Yenisei-Khatanga basin). Thus, according to thermometric measurements in wells, the permafrost thickness is about 500 m within the Paiyakha oil field. At this, the resistivity logs and MT sounding results show that in the upper 200 meters of the section deposits are completely in the frozen state (permafrost), inasmuch as the resistivity values exceed 30 Ohm·m (Fig. 7). The drilling results revealed that at depths below 200 m deposits are essentially clayey.

The dependence of the thickness of high resistivity layer, which is associated with permafrost deposits, on their lithology can be remarkable, if the geoelectric sections are overlapped by seismic sections. This comparison is exemplified by the principal lithological-geophysical model shown in Fig. 8, *a*, *b*, indicating that the localities with increased permafrost thickness in the center of the section, above the Rassokha megaswell, and in the south, on the slope of the Dudypta megatrough, are consistent with the layer (as it approaches the surface) discriminated on the seismic section. The observed higher resistivities

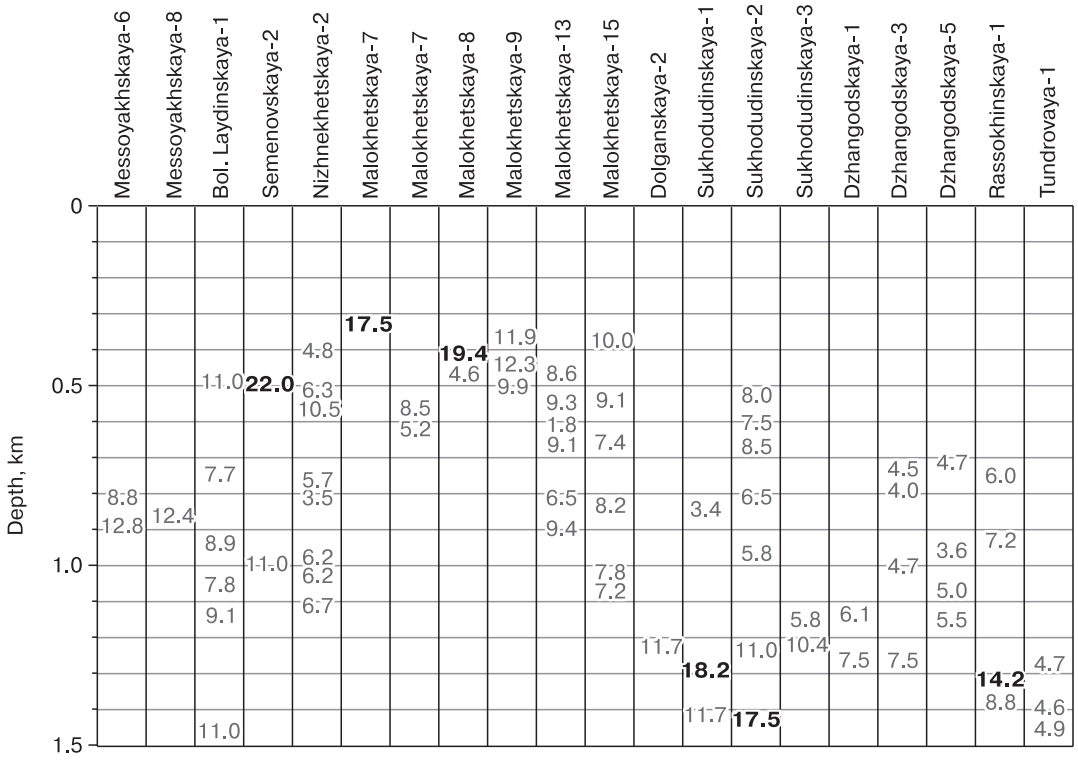

Fig. 5. TDS values for pore water solutes in the study area from the results of well tests.

The values in a bold font exceed 14 g/L, the rest are less than 14 g/L.

(17–30 Ohm·m) in this layer below the permafrost base attest to the dominance of sandstones. This conclusion is inferred from the results of the well data interpretation [*Afanasenkov and Yakovlev, 2018*] and is consistent with the general understanding of sandy-clayey deposits resistivity patterns at pore water salinity less than 12 g/L [*Ryzhov and Sudoplatov, 1990*]. The layer resting on sandstones is composed of mainly clays judging from the lower resistivity values. The deposits of this layer therefore retain bound water whose freezing point is as low as –2...–3 °C. Even though the clayey layer yields to freezing under the action of lower temperatures at depths of 0–200 m, however its resistivity is lower (100–200 Ohm·m) than that of the sand layer (300–500 Ohm·m [*Osterkamp, 2001*]). Similar sites of locally increasing permafrost thickness are observed in the section along Line 2 (Fig. 8, *c*). Accordingly, distinctive features of the permafrost strata visible on Line 3 in the geoelectrical section (Fig. 8, *d*) also can be explained by the structural and lithological characteristics.

Specific features of the permafrost strata structure. Extensive areas with significantly increased permafrost thickness are characteristic of the study region, which is probably associated with the sediment composition. Of them, one zone is located in the eastern portion of the Yenisei-Khatanga basin, to the north of the Khatanga river. The section along Line 4 crossing this zone is shown in Fig. 8, *e*. The upper part of the section is likely to be composed there of thick sand layers capable of freezing up to a depth of 1 km. The lower boundary of the high-resistivity layer is "blurred", with no sharp transition to the underlying conductive deposits observed in other places. This allows to assume that in the unfrozen state, deposits composing this sand layer have higher resistivity. However, both the northern and southern endings of this layer (where it is overlain by permafrost depos-

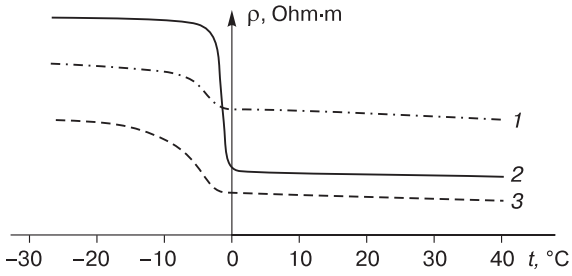

Fig. 6. Type of a relationship between electrical resistivity (ρ) of water-saturated rocks and temperature [*Ogil'vi, 1990*].

1 – rocks (ρ_r); *2* – sands (ρ_s); *3* – clays (ρ_c).

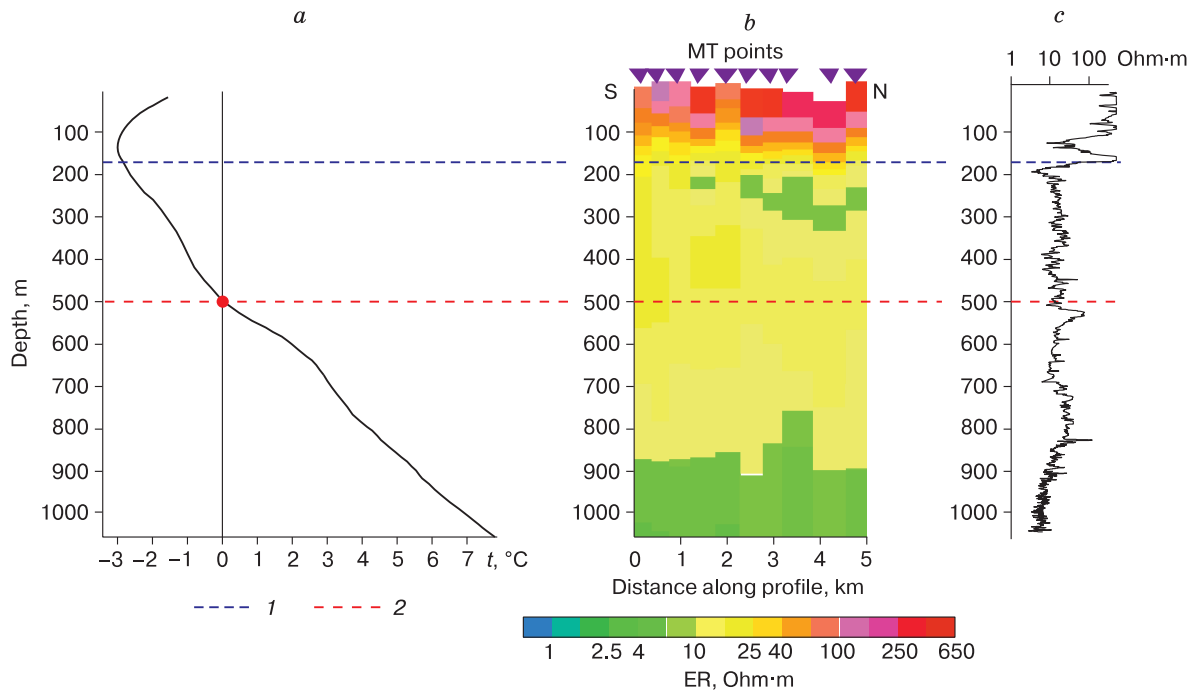

Fig. 7. Position the permafrost base (*1*) and permafrost zone (*2*) in the area of Paiyakhskaya-1 well located in the west of the study area.

a – temperature curve for Paiyakhskaya-1 well; *b* – a fragment of a geoelectrical section along Profile 501 of Novotaimyrskaya area; *c* – electrical well log (WL) in Paiyakhskaya-1 well. The position of the base is determined from WL (*1*) and t = 0 °C (*2*).

its) exhibit a significant decrease in its resistivity. As such, the increase in resistivity in the sandy reservoir beneath the permafrost layer is accounted for the accumulation of gas or gas hydrates, with permafrost acting as a caprock. (Discussed below in greater detail.)

Among other characteristic features inferred from the regional electromagnetic studies, the permafrost structure is represented by conducting zones of different types. Figure 9 shows two examples of the presence of layers with very low resistivity (<2–3 Ohm·m) identified beneath the permafrost, while other similar zone are remarkably discriminated on the sections in Fig. 8. Its low resistivities are most likely caused by higher salinity of pore water solutes. The enhanced salinity beneath the permafrost layer may be associated with salts expulsion into the underlying layers during the sediment freezing [*Romanovsky, 1983; Ershov, 2002*].

As is the case with the zone of continuous melting occurring under large riverbeds, the conducting zones of another type largely disable homogeneity of the permafrost strata (Fig. 8, *e*, 9). For example, a zone of partial melting is localized beneath the Khatanga river (the southern end of the section along Line 4). In the same section, along Line 4, a local zone of lower resistivity is marked in the lower part of permafrost. Such areas are observed in places where the thickness of permafrost is more than 500 m. As such, the conducting zones within the permafrost strata are associated probably with large tectonic dislocations and a specific fluid flow in them, the one driven by the influx of warmed aqueous solutions ascending from the depths.

All these examples show the electrical prospecting technique applications are appropriate not only for investigations of regional characteristics of permafrost, but are also helpful in revealing local heterogeneities in them.

Map of the permafrost base depth in the northern margin of the Siberian platform

All the profiles, along which the electrical prospecting surveys have been carried out since 2005, show the base of a high-resistivity layer, which, as was discussed above, is interpreted by the authors as permafrost deposits (in the frozen state), whose base (lower boundary) is distinctly visible on the geoelectric sections. In most of the study area, the position of the base is unambiguously determined by a sharp change in resistivity from 10–30 to 150–300 Ohm·m in the adjacent layers. While in some parts of the profiles, variations of electrical resistance with depth show a smoother pattern. In such zones, the base of the layer was determined from the boundary values of resistivity 50–80 Ohm·m (the mean geometric value

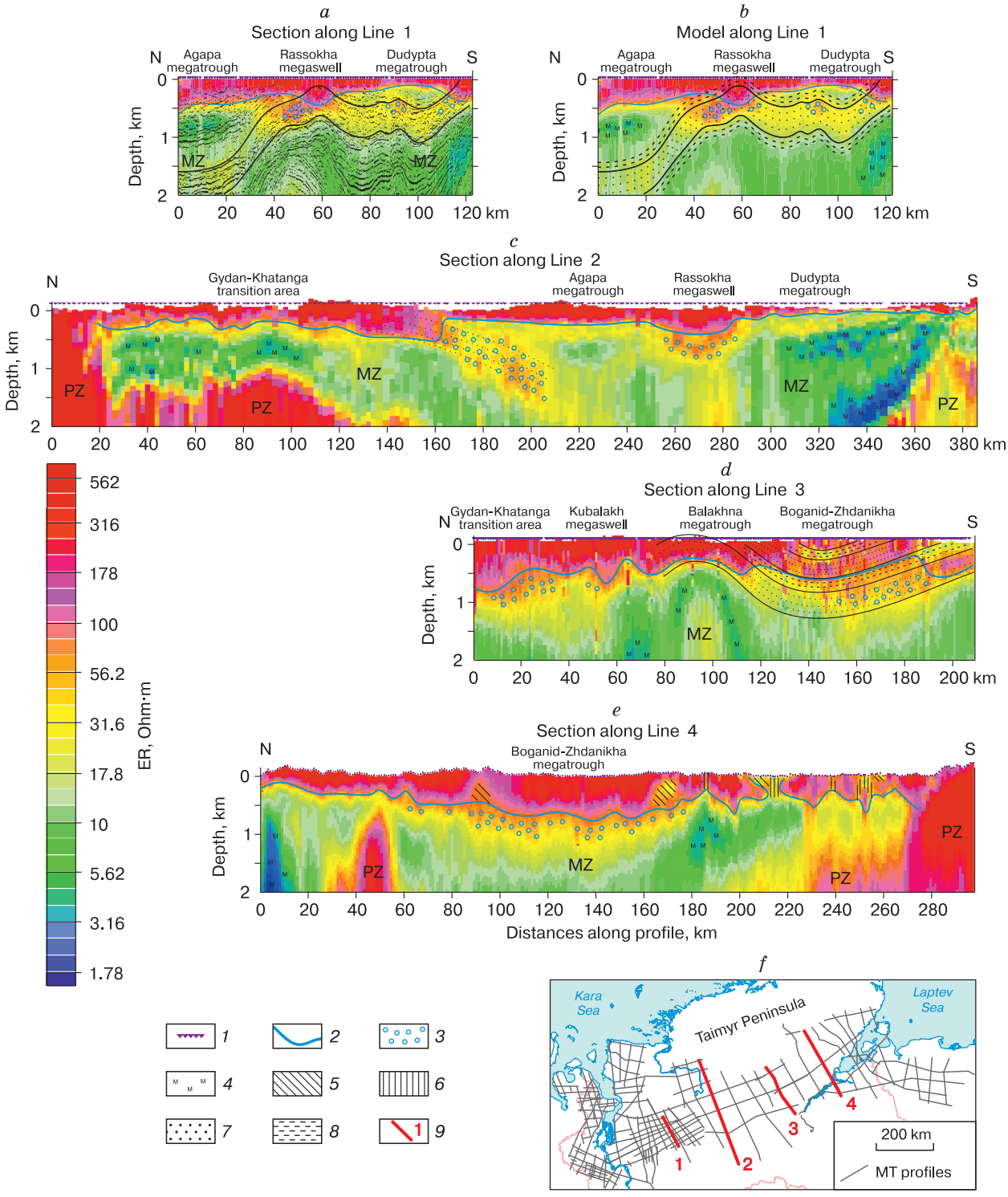

Fig. 8. Geological and geophysical sections of roughly N–S direction to a depth of 2 km.

a – combined geoelectric and seismic sections along Line 1; *b* – geological model along Line 1; *c–e* – geological and geophysical sections along Lines 2–4, respectively; *f* – regional electric prospecting profiles scheme for the study area. Geological complexes: PZ – Paleozoic, MZ – Mesozoic. *1* – MT sounding points; *2* – permafrost limit; *3* – subpermafrost high-resistivity anomalies; *4* – subpermafrost lower resistivity zones; *5* – zone of partial melting; *6* – zone of continuous melting; *7* – sandy deposits; *8* – clayey deposits; *9* – position and number of cross-section lines in the schematics.

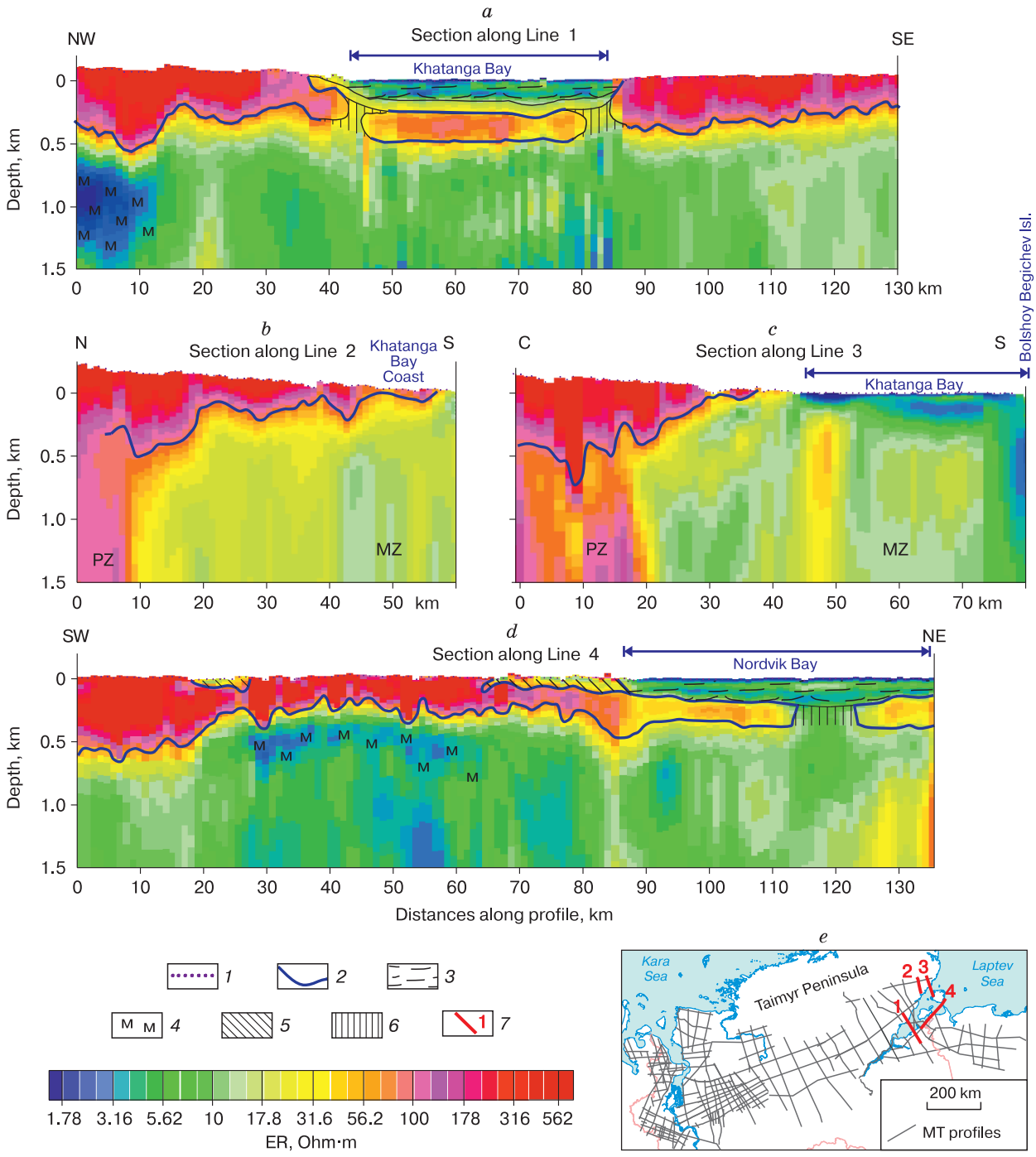

Fig. 9. Geoelectric sections of the upper 1.5 km along the profiles in the Khatanga Bay area (MT soundings were carried out from the ice in the offshore areas).

a–d – geological and geophysical sections along Lines 1–4, respectively; *e* – scheme of regional electric resistivity prospecting profiles of the study area. Geological complexes: PZ – Paleozoic, MZ – Mesozoic. *1* – MT sounding points; *2* – border of permafrost; *3* – unfrozen layer beneath the waters; *4* – lower resistivity zone overlain by permafrost; *5* – zone of partial melting; *6* – the zone of continuous melting; *7* – position and number of section lines in the diagram.

of resistivity for two layers at the base of the high-resistivity layer in the case of a contrast boundary). These values correlate with the well log data (Fig. 4).

The results and findings enabled generation of a map of the permafrost base depth (Fig. 10), which showed that in localities where permafrost deposits

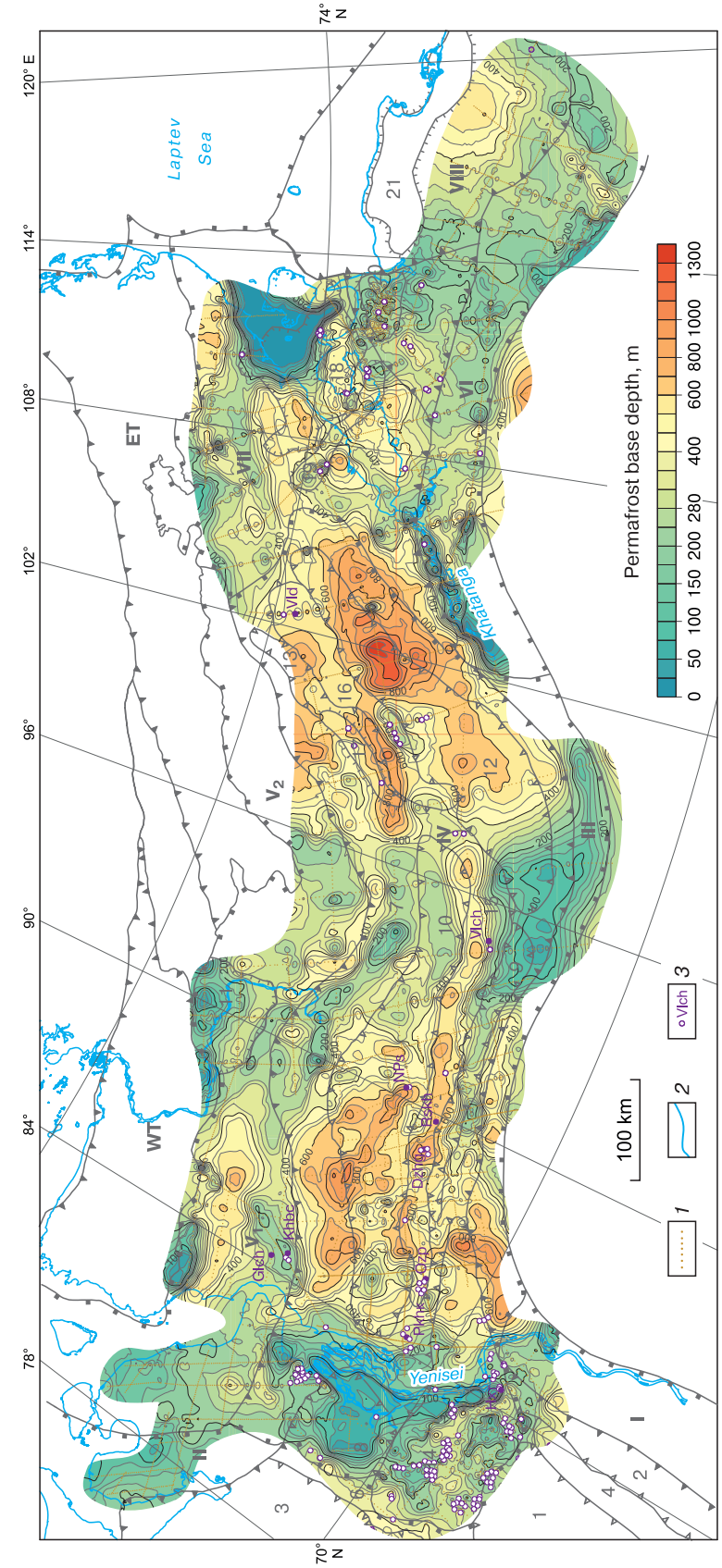

Fig. 10. Map of the permafrost base depth according to MT soundings.

1 – MT sounding points; 2 – coastline; 3 – deep wells: Dzhg – Dzhangodskaya-4, NPs – North-Pyasinskaya-1, Phk – Paiyakhskaya-1, Vld – Vladimirskaya-21, Nzht – Nizhnekhetskaya-1, Vlch – Volochanskaya-2, Ozr – Ozernaya-2, Rskh – Rassokhinskaya-1, Khbs – Khabeyskaya, Glch – Golchikhinskaya. For other notations see Fig. 1.

outcrop onto the surface, the numerical symbols on the map coincide with the thickness of permafrost; in places where permafrost is onlapped by the unfrozen layer (for example, in offshore areas), the permafrost thickness is less than the base depth of that layer. In permafrost-free zones, the base depth of this layer is indicated by zero. The length of the profiles used totals over 20 000 km (about 22 000 points of MT soundings). The observation network being non-uniform, this resulted in different scales of the constructed maps: 1:200 000 for the western parts, 1:500 000 for the eastern parts, and 1:1 000 000 for the central parts. The presented map has a scale factor of 1:1 000 000. Despite its small scale, the authors believe this map to be ranked today as the most reliable and detailed source of information about the permafrost base depth in the region, which is indicative of the regional patterns of changes in the permafrost strata thickness.

The accuracy of determinations of the permafrost thickness from the MT sounding data depends on the contrast between its resistivity and that of the underlying deposits. In most cases, high contrast allows estimating accuracy up to 5–7 % of the depth. This means that for 50 m thickness the error is ±3 m and will be, accordingly, ±30 m for 500 m. These values serve the basis for selecting the spacing between isolines.

Permafrost thickness tends to decrease and ranges from 0 to 150 m in the west of the area near the Yenisei river, in the transition area to the West Siberian platform. The zone of reduced thickness elongated in the N–S direction, stretches along the Yenisei river.

As the permafrost-underlain area advances further eastwards (within the Dudypta and Agapa megatroughs area and Rassokha megeswell), its thickness increases. The permafrost thickness reaches maximum (up to 900 m) to the north from the axial part of the Agapa megatrough, at the Yenisei and the Pyasina interfluve. Additionally, the elevated permafrost thicknesses (500–700 m) are characteristic of the Rassokha megeswell area. The southern margin of the study area is marked by local increase in permafrost thickness, up to 1000 m in the transition region of the Siberian platform to the Yenisei-Khatanga regional trough. In the north, the observed roughly W–E elongated area of bigger thicknesses of permafrost corresponds to the central part of the South Taimyr monocline in the area where Khabeyskaya and Golchikhinskaya wells are located. Whereas the Dudypta megatrough is differentiated by a lower thickness of the underlying permafrost (100–300 m).

The thickness of permafrost tends to decrease in the central part of the study area, averaging 200–400 m. The correlation between changes in permafrost thickness and the position of the major structural and tectonic elements of the Yenisei-Khatanga basin persists. The permafrost thickness decreases down to 50–100 m in the zone above the Dudypta megaswell transient into the Boganid-Zhdanikha megatrough, while the Gydan-Khatanga transition zone is also characterized by reduced magnitude of permafrost thickness (100–300 m). The zone of increased (up to 400–500 m) permafrost thickness surrounding the Yangoda-Gorbit uplift can be traced westwards, as far as the Yenisei Bay. This is likely to be associated with its approaching the surface of essentially sandy layer, similarly to the site lying between 120 and 160 km of the section along Line 2 (Fig. 8).

The eastern part of the Yenisei-Khatanga basin is characterized by thick underlying permafrost (500–800 m). The Balakhna megaswell and the Kubalakh swell are marked by shallower base depth (350–500 m) of permafrost (the section along Line 3, Fig. 8). The area between the swells is interpreted as a strip with increased permafrost thickness (800–900 m). While the magnitude of the permafrost thickness is anomalously high (>1000 m) within the eastern closure of the Boganid-Zhdanikha megatrough, whose northeastern part is in full characterized by permafrost thickness exceeding 800 m.

The eastern part of the study area has no explicit anomalies, with the magnitude of permafrost thickness interpreted as: moderate (350–500 m) in the Anabar-Khatanga upfold (saddle); lowered (200–300 m) within the Anabar monoclise and the Lena-Anabar basin; the lowest (in the Anabar river valley). Beneath the Khatanga Bay, the permafrost thickness is ranked as minor and can have zero values.

Permafrost underlying the Khatanga Bay

Given that in the east of the study area, some of the MT sounding profiles were laid across the Khatanga Bay, the measurements were made from the ice. The magnetic field was recorded by ice surface-based induction sensors, while the electrical field was measured using special electrodes located in the holes drilled in the lower part of the ice cover.

The data obtained enabled a pioneering comprehensive study of the permafrost structure in the offshore part of the bay. Measuring the permafrost thickness in the Khatanga Bay is now of great practical importance for the launched drilling operations there to be continued. The information about the occurrence of permafrost, and position of its upper and lower boundaries is critical for the drilling platform construction in the Khatanga Bay.

Figure 9 shows geoelectric sections derived from the MT sounding data to a depth of 1.5 km along the section of the profile crossing the Khatanga Bay (Fig. 9, *a*), on the northern shore of the Khatanga Bay (Fig. 9, *b*, *c*) and through the Nordvik Bay (Fig. 9, *d*). MT soundings are spaced 1 km apart on the profile. The sections are derived from the results of automatic one-dimensional inversion on the effective MT sounding curves.

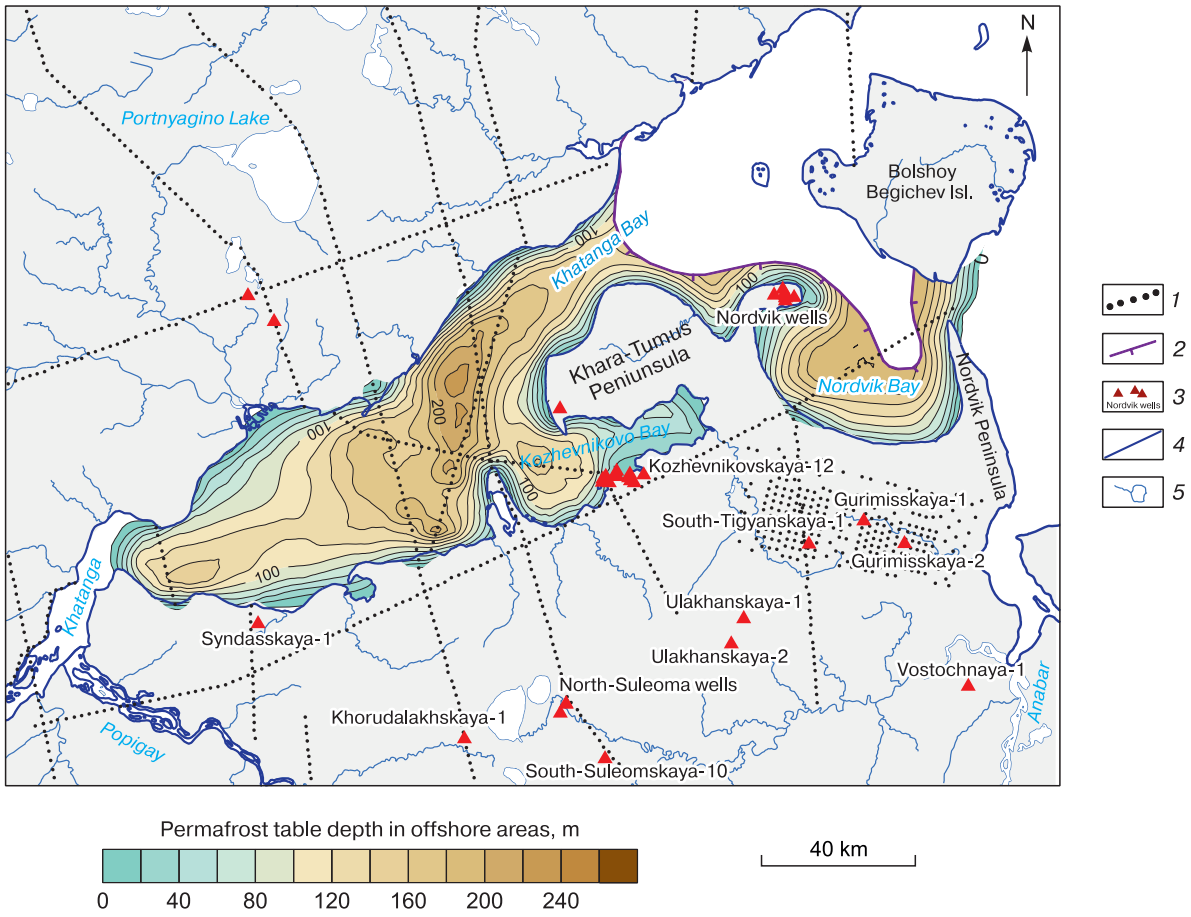

Fig. 11. Map of the permafrost table position in the Khatanga Bay offshore area.

1 – MT sounding points; *2* – pinch out boundary of permafrost; *3* – deep wells and their names; *4* – coastline; *5* – rivers and lakes.

Fig. 9, *a* shows that in the upper part of the section (onshore part of the profile) permafrost thickness is 300–500 m; the areas of lower resistivity in the coastal zones of the Khatanga Bay are apparently associated with taliks. It should be noted that this inference requires more detailed studies in the coastal zone.

Given that deposits occurring beneath the Khatanga Bay in the upper part of the section experienced thawing, their resistivity is low and not more than 10 Ohm·m to a depth of 150–200 m. The layer of permafrost deposits beneath the bay with a thickness of 200–250 m has lower resistivity, than in the onshore part (30–100 Ohm·m).

In the study of permafrost in the offshore area, the biggest challenge was created by the screening properties of the water layer and the upper layer of deposits in the unfrozen state (Fig. 9, 11), whose effect significantly reduced the data sensitivity to the permafrost parameters. The results nevertheless suggest the presence of subaqueous permafrost layer and allow to estimate the depth of its top and base (Fig. 11). The submarine permafrost is found totally missing both in the northeastern part of the Khatanga Bay (Fig. 9, *b*, *c*), and in the central part of the Nordvik Bay (Fig. 9, *d*).

Despite the irregular character of the existing measuring network performance, there are reasonable grounds for believing that the permafrost underlies the rest of the Khatanga Bay. This interval has a number of features:

– a low resistivity layer (from 3 to 10 Ohm·m) resting on the permafrost is the layer of deposits in the unfrozen state, with the thickness ranging from 50 m near the bay coast to 150–200 m in its central part. As is the case with the layer of water, its high conductivity provide additional challenges in the electrical resistivity prospecting applied to investigations of the high-resistivity permafrost beneath it;

– the permafrost layer shown on the geoelectric section is noted for resistivities lower than onshore (from 20 to 70–100 Ohm·m). The thickness of this high-resistivity layer varies from 100 to 300 m. The base depths of the layer varies from 340 to 570 m;

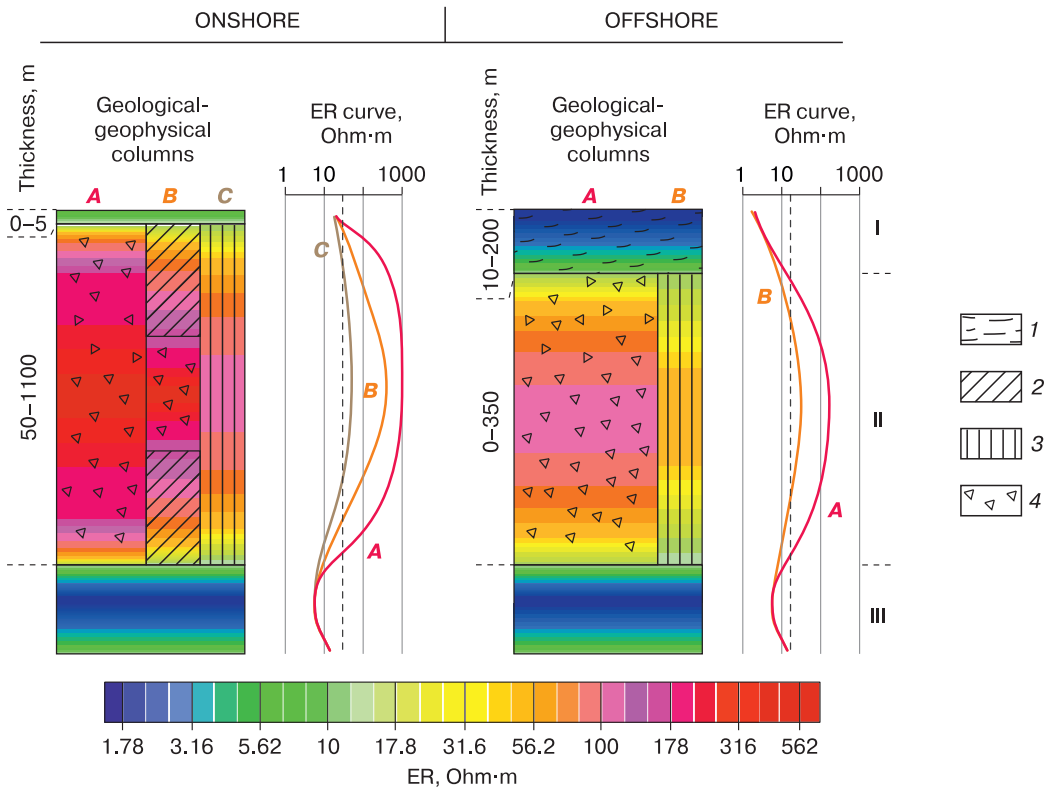

Fig. 12. Generalized geoelectrical characteristics of the shallow subsurface section of the study area.

I – unfrozen layer in the upper part of the section; II – permafrost layer; III – underlying Jurassic-Cretaceous terrigenous deposits. *1* – unfrozen layer beneath the body of water; *2* – zones of partial thawing; *3* – zones of continuous thawing; *4* – deposits in the frozen state.

– on all the profiles crossing the western part of the Khatanga Bay, the permafrost bed contains through-the-thickness zones with lower resistivities, of which most are observed at the water-to-land transition boundary;

– screening properties of the water layer and the unfrozen bed resting on the permafrost deposits worsen the accuracy of determination of subaqueous permafrost parameters, which is lower as compared to the onshore parts. This is corroborated by the average accuracy of determinations of the permafrost base depth: 5–7 % of the thickness for the onshore permafrost versus 15–20 % of the permafrost strata thickness for the offshore area. The greater is the thickness of the screening layers (primarily, the layer of water), the lower is this parameter, inasmuch as its resistance is an order of magnitude less than that of the layer of deposits in the unfrozen state.

The presented MT soundings results have demonstrated good prospects of electrical resistivity measurements for the permafrost studies both in the onshore/offshore areas and in the transition zones, which appears a very important practical task from the perspective of the Arctic shelf development.

The summary of results of the electrical resistivity prospecting studies enabled characterization of geoelectric properties in the upper part of the section of the study area, which is imaged in Fig. 12, separately for onshore and offshore areas, differentiating primarily by the presence of topping unfrozen layer, and by the contrasting resistivity values for permafrost. These characteristics can serve as an a priori information about the study region either for the purposes of further electrical exploration or numerical modeling.

High resistivity anomalies in the subpermafrost layer

The first MT soundings in 2015 in the west of the study area were conducted with a spacing of 500 m along the profile, with the profiles passing through the known Paiyakh, Baikalovsk and Ozernoe oilfields. The interpretation results of the resistivity data obtained for the shallow subsurface overlying them, revealed a pattern characterized by zones of high-resistivity anomalies in the upper part of the section within the 300–800 m depth interval beneath the permafrost stratum [*Afanasenkov et al., 2015*].

Figure 13 shows a geoelectric section along one of the profile laid in 2015 in the western part of the Yenisei-Khatanga basin, on the right bank of the Yenisei river, and passing through the Paiyakha and Baikalovsk oilfields. The high resistivity anomalies (HRA) localized beneath the permafrost are discriminated in the section, with gas hydrate accumulations being the most likely explanation for these anomalies [*Waite et al., 2009*]. Given these thermobaric conditions, a gas hydrate stability zone (GHSZ) is located specifically at depths of 300–800 m. The mechanism of gas hydrate formation and accumulations within this depth interval has been discussed in many works [*Makogon, 2010; Sivtsev and Rozhin, 2011*]. Some publications [*Yakushev, 2009*] mark the appearance of intermediate zone sandwiched between the permafrost and GHSZ, which is differentiated in the section by the resistivity lowering at depths of 200–300 m. Such a conductive strip distinctly partitions the subpermafrost HRAs from the permafrost stratum, which is favored by small thickness of permafrost: from 150–200 m (permafrost base depth) to about 300 m (top of GHSZ). Accordingly, anomalies of this type can be commonly observed in the areas where permafrost thickness is less than 250–300 m. These include the entire Yenisei-abutting stretch of the Yenisei-Khatanga basin, the south-western part of the Boganid-Zhdanikha megatrough, the Anabar river valley, as well as some smaller-size zones (Fig. 10).

The anomalies of the kind are termed isolated, or the first type HRAs (Fig. 14, I) characterized by: a lower resistivity layer confidently separating the anomalies from the permafrost stratum; subhorizontal structure of the background section and, accordingly, the absence of resistivity anomalies associated with the structural and morphological factor in the upper part of the section.

In the case of the permafrost base occurring below the top of the GHSZ, the subpermafrost anomalies associated with HC accumulation at greater depths will underlie the permafrost stratum. Similar anomalies were detected above the Ozernoe oilfield. They are termed added (apparent) and are assigned to the second type (Fig. 14, II). Figure 14 shows a

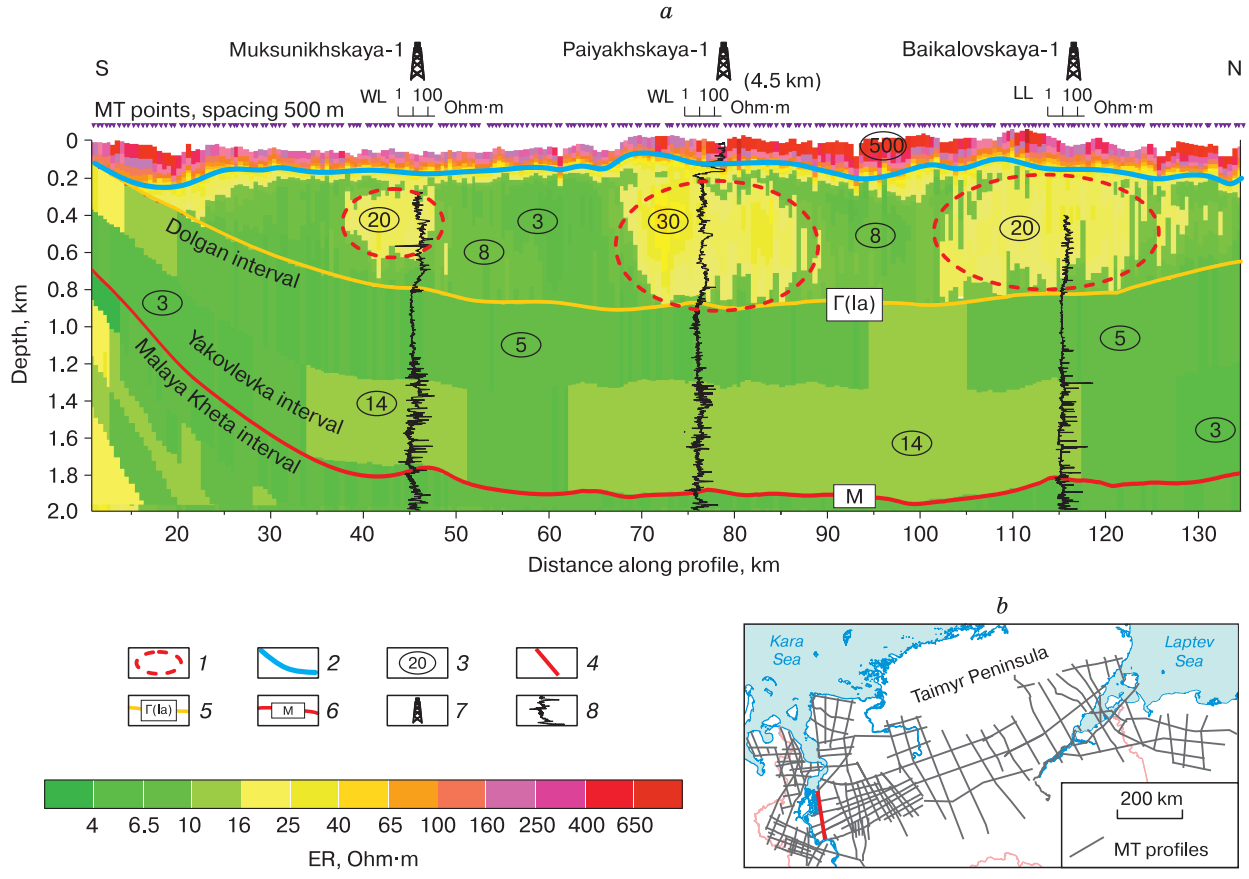

Fig. 13. Geoelectric section of the uppermost 2 km with subpermafrost high-resistivity anomalies along Profile 501 in the west of the Yenisei-Khatanga basin (*a*) and scheme of regional electrical prospecting profiles for the study area (*b*).

1 – subpermafrost high resistivity anomalies; *2* – permafrost base according to the resistivity surveys; *3* – average resistivity value for the layer; *4* – profile position on the diagram; *5*, *6* – seismic horizons and their indices (*5* – top of the Upper Cretaceous Dolgan Formation, *6* – top of the Lower Cretaceous Neitin (Koshai) clayey unit; *7* – deep wells; *8* – electrical well logs.

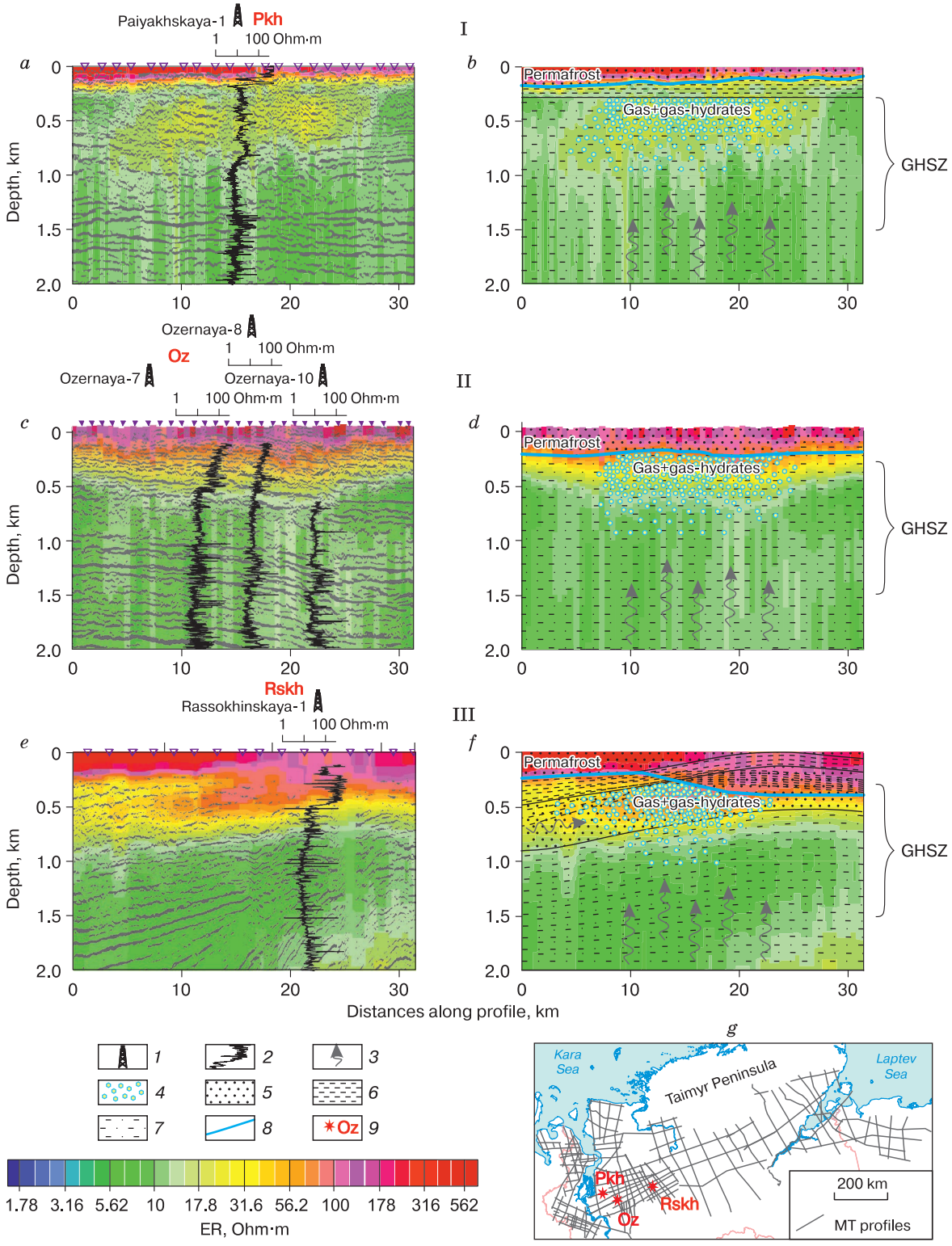

Fig. 14. Three types of permafrost anomalies of increased electrical resistivity (I–III).

a, *c*, *e* – seismic and combined geoelectric sections in the area of locations of wells: Paiyakhskaya wells (Pkh), Ozernaya wells (Oz), *e* – Russokhinskaya well (Rskh); *b*, *d*, *f* – corresponding geological-geophysical models; *g* – regional electrical prospecting profile of the study area. *1* – deep wells; *2* – electrical well logs; *3* – direction of hydrocarbon migration; *4* – accumulations of gas and gas hydrates; *5* – sandy deposits; *6* – clayey deposits; *7* – sandy-clayey deposits; *8* – permafrost base; *9* – borehole position and its index on the scheme. GHSZ – gas hydrate stability zone.

remarkable local increase in the permafrost thickness, while its lower boundary is blurred.

The reason may be due to the water in pore spaces is replaced by gas or gas hydrates. The relatively local nature of the anomaly can be explained by a weak horizontal permeability of the layers within the shallow subsurface interval. The HRA contours in this case will nearly closely delineate the HC accumulation occurring deeper down. The characteristic features of type two anomalies are: a local increase in the permafrost stratum thickness not associated with structural factors; the blurred lower boundary of the permafrost bed in the geoelectric sections.

The third type of anomalies is established above the Dzhangoda HC accumulation on the Rassokha magaswell where the reservoir sand layer overlying the domed portion approaches the surface and falls into the zone of negative temperatures, with the free pore moisture in this layer subjected to freezing, sealing thereby the pores. At this, the permafrost base occurs deeper below. Upon freezing, the water plugs up the pores in the reservoir layer, making the frozen interval impermeable (a seal). The migrating up the slope hydrocarbons can accumulate in the reservoir layer in its parts approaching the arch, "corked" by the frozen deposits. Due to the HC accumulating within the slope parts of the reservoir bed occurring beneath the permafrost its resistivity increases to 30–100 Ohm·m (Fig. 14, III) against the backdrop of 17–30 Ohm·m in the deep buried zones. This type of anomalies is interpreted as structural-morphological. The allocation of such structural and morphological gas and gas hydrate accumulations has been addressed to in a muber of works (e.g. [*Polozkov et al., 2011*]). The characteristic features of type three HRAs are: the presence of local zones of increased permafrost thickness due to the structural factor; an increase in resistivity of the subpermafrost sandy reservoir bed.

Anomalies of all the discussed three types were identified in all the sections of the study region. Almost all known hydrocarbon fields correspond to subpermafrost anomalies of increased resistivity type I, since most of the HC fields are concentrated in the west of the study area, where permafrost thickness is relatively small. It is remarkable that at least part of the gas or gas hydrates accumulations in the drilled areas could have formed due to the gas-liquid annular flows. Such possibility has been provided insights about in some works [*Sivtsev and Rozhin, 2011*].

While allocation of type one HRAs appears not to be a problem, it is difficult to distinguish between the second and third type anomalies, exactly those specifically relating gas hydrate accumulations, which is due to the fact that, as shown above, a local increase in permafrost thickness may have been caused by changes in the lithological characteristics of deposits. The blurred boundary of the permafrost base can be explained by the dominating sandstones being gradually replaced by clays. At this, confident allocation of type three anomalies requires the knowledge of the depth of permafrost penetration to differentiate zones of the increased resistivity caused by the sediment freezing, from those which are associated with HC accumulations.

It should also be noted that subpermafrost HRAs of the first and second types are confined to the HC accumulations emplaced immediately below them, while the sources of the third type anomaly may be located away from the anomaly itself, given that HC are capable of migrating along the corresponding reservoir layer due to its high lateral permeability and inclined bedding.

Summing it all up, we ascertain that the presence of such subpermafrost anomalies of increased resistivity can be interpreted as one of indications of potential target for search for deep-seated HC accumulations, with the opportunities opening up for:

1. ***Prediction of oil and gas potential.*** The direct correlation of the anomalies detected in the shallow subsurface with commercial development of hydrocarbon accumulations in the underlying pay zones allows using these anomalies for the prediction of HC accumulations in deep-seated horizons.

2. ***Delineation of hydrocarbon accumulations.*** In areas with subhorizontal occurrence of layers and subvertical tectonic disturbances in the upper part of the section HC migration occurs mainly in the vertical direction. It can therefore be assumed that there is some correlation between the contours of high-resistivity anomalies and of the deep-seated HC accumulations.

3. ***Revealing areas of engineering-geological hazards, prediction of complicated zones while drilling.*** It stands to reason that gas/gas hydrates accumulating under the permafrost layer, when released, can cause destruction of the engineering structures erected on the surface. The resulting anomalies can mark the segments in the section hazardous for drilling.

CONCLUSIONS

The regional studies using the integrated geophysical methods applied to the northern margin of the Siberian platform (commenced in 2005 and is currently ongoing) have provided new data on the geological structure of the study region [*Afanasenkov et al., 2018*]. The results of electrical prospecting as part of the comprehensive geophysical methods, allowed accumulating a large amount of new information about the permafrost structure. Based on the results presented herewith, the following conclusions can be drawn.

1. MT and TEM soundings are electrical prospecting methods which enable a reliable allocation of a contrasting high-resistivity layer in the upper part of the section, which the authors interpret as the interval of deposits in the frozen state, as well as the

allocation of local inhomogeneities within this layer (taliks, local zones with variations in thickness).

2. Part of the deposits within the permafrost strata being in the cooled state (despite their negative temperatures, pore water solutes remain unfrozen), these therefore do not differ from the resistivity of the underlying sediments. The predominantly clayey deposits containing bound water in the pores in this interval is the main reason for the presence of unfrozen pore water solutes in the zone of negative temperatures. The permafrost zone thickness within the Yenisei-abutting stretch determined from the borehole temperature-depth profiles is therefore significantly greater than of frozen deposits thickness inferred from the electrical prospecting data.

3. The structural and lithological features of the section represent major controls determining the pattern of permafrost thickness variations across the study region.

4. The constructed map of the base depth of permafrost, based on a large amount of actual material, reflects the regional patterns of distribution of this bed. The thickness of permafrost is the lowest in the Yenisei and Khatanga rivers valleys (locally, less than 20 m), and the largest (more than 1000 m) on the eastern closure of the Yenisei-Khatanga basin.

5. The MT sounding data allowed to establish that permafrost is absent from the northeastern part of Khatanga Bay and the center of the Nordvik Bay. In the west of the Khatanga Bay and in the coastal part of the Nordvik Bay permafrost thickness is about 350 m. A layer of deposits in the unfrozen state (thickness: up to 200 m) found resting on the permafrost stratum is in the center of the offshore areas.

6. The distinguished subpermafrost anomalies of increased resistivity are grouped into three types. The correlation between the anomalies and known hydrocarbon fields allows to relate these anomalies to the accumulation of gas hydrates and free gas within the subpermafrost layer.

The authors express their most sincere gratitude to V.E. Tumskoy, A.P. Afanasenkov, E.P. Shirokova, D.G. Kushnir for their help in preparing our manuscript for publication, as well as to E.Yu. Sokolova and I.N. Modin for the review.

References

Afanasenkov, A.P., Obukhov, A.N., Chikishev, A.A., et al., 2018. Tectonics of northern margin of the Siberian Platform from the comprehensive analysis of geological and geophysical data. Geologia Nefti i Gaza, No. 1, 7–27.

Afanasenkov, A.P., Volkov, R.P., Yakovlev, D.V., 2015. High electrical resistivity anomalies in deposits underlying permafrost as new indication of hydrocarbon accumulations. Geologia Nefti i Gaza, No. 6, 40–53.

Afanasenkov, A.P., Yakovlev, D.V., 2018. Application of electrical prospecting methods to petroleum exploration on the northern margin of Siberian Platform. Geologia i Geofizika (Russian Geology and Geophysics) 59 (7), 1029–1049.

Ageev, V.V., Ageev, D.V., 2017. The study of permafrost cross-sections in Yakutia using TEM and VES-IP methods. Inzhenernaya Geologia, No. 2, 64–69.

Baranov, M.A., Kompaniets, S.V., Buddo, I.V., et al., 2014. Applications of electromagnetic soundings to subsurface permafrost mapping. Vestnik IrGTU 7 (90), 25–30.

Berdichevskii, M.N., Dmitriev, V.I., 2009. Models and Methods of Magnetotellurics. Nauchny mir, Moscow, 680 pp. (in Russian)

Constable, S.C., Parker, R.L., Constable, C.G., 1987. Occam's inversion – A practical algorithm for generating smooth models from electromagnetic sounding data. Geophysics, No. 52, 289–300.

Ershov, E.D., 2002. General Geocryology. Moscow University Press, Moscow, 682 pp. (in Russian)

Khmelevskoy, V.K., Kostitsin, V.I., 2010. Basics of Geophysical Methods. Perm University, Perm, 400 pp. (in Russian)

Khmelevskoy, V.K., Modin, I.N., Yakovlev, A.G. (Eds.), 2005. Electrical Methods: a Guide for Electric Survey Practice for Students majoring in Geophysics. GERS, Moscow, 311 pp. (in Russian)

Koziar, A., Strangway, D.W., 1975. Magnetotelluric sounding of permafrost. Science, No. 190 (4214), 566–568.

Koziar, A., Strangway, D.W., 1978. Permafrost mapping by audiofrequency magnetotellurics. Can. J. Earth Sci., No. 15 (10), 1539–1546.

Makogon, Yu.F., 2010. Gas Hydrates. History of study and prospects for development. Geologia i poleznye iskopaemye Mirovogo okeana, No. 2, 5–21.

Nim, Yu.A., Omelyanenko, A.V., Stognii, V.V., 1994. Electromagnetic Induction Resistivity Surveys in Permafrost. OIGGM SO RAN, Novosibirsk, 189 pp. (in Russian)

Ogil'vi, A.A., 1990. Fundamentals of Engineering Geophysics. Nedra, Moscow, 501 pp. (in Russian)

Osterkamp, T.E., 2001. Sub-sea permafrost, in: Encyclopedia of Ocean Sciences. Acad. Press, N.Y., p. 2902–2912.

Polozkov, A.V., Astafiev, D.A. Istomin, V.A., et al., 2011. Detection of gas hydrate zones in low-temperature deposits when constructing wells and expected types of gas-hydrate deposits. Vesti Gazovoy Nauki 3 (8), 78–86.

Romanovsky, N.N., 1983. Underground Waters in Permafrost. Moscow University Press, Moscow, 231 pp. (in Russian)

Ryzhov, A.A., Sudoplatov, A.D., 1990. Conductivity calculations of sand-clays the use of functional dependences for solving hydrogeological problems, in: Scientific-technical achievements in geology and subsurface prospecting. VIEMS, Moscow, pp. 27–41. (in Russian)

Sivtsev, A.I., Rozhin, I.I., 2011. Unconventional impermeable permafrost seal of hydrate origin, in: Proceedings of The International Engineering Permafrost Conference, NPO Fundamentstroiarkos OOO, Tyumen, pp. 138–142. (in Russian)

Sternberg, B.K., Washburne, J.C., Pellerin, L., 1988. Correction for the static shift in magnetotellurics using transient electromagnetic soundings. Geophysics, No. 53 (11), 1459–1468.

Waite, W., Santamarina, J., Cortes, D., et al., 2009. Physical properties of hydrate-bearing sediments. Rev. Geophysics, vol. 47, RG4003, DOI: 10.1029/2008RG000279.

Yakupov, V.S., 2008. Geophysics of the Permafrost. Izdat-vo Yakutskogo un-ta, Yakutsk, 342 pp. (in Russian)

Yakushev, V.S., 2009. Formation and accumulation of natural gas and gas hydrates in the permafrost. Dissertation, to obtain the degree of Doctor Sci. in geol.-mineral., Moscow, 249 pp. (in Russian)

Zykov, Yu.D., 1999. Geophysical Methods of Permafrost Studies. Moscow University Press, Moscow, 243 pp. (in Russian)

Received January 31, 2018